JOURNAL OF MATERIALS SCIENCE 25 (1990) 2562–2568

Loss of precious metal from Pt–Rh alloy under refractory oxide environments

T. C. CHOU, A. MISHRA, D. ANDERSON
Research and Development, Engelhard Corporation, Edison, New Jersey 08818, USA

Loss of precious metals from a Pt–10 wt% Rh alloy was studied at 1300° C in refractory oxides and fused quartz environments. After 60 and 150 h annealings, samples exposed to gaseous environments showed significant weight loss. The surface was attacked and characterized by micron-sized pits, as well as river-like striations. The pits were found to be enriched with silicon and/or aluminium depending upon the heating environment. Laser Raman microprobe identified that the major compound formed in the pits is α-cristobalite.

Direct solid state contact of Pt–Rh with Al_2O_3 and SiO_2 showed interactions between materials. The interaction was more extensive between Pt–Rh with SiO_2 than with Al_2O_3. On the other hand, no evidence of interaction except pitting and striation was observed on Pt–Rh when exposed to a vapour environment.

The presence of pits and striation patterns indicated that refractory oxides attacked Pt–Rh under atmospheric conditions, and gave rise to the weight loss. Calculation of weight loss by an oxidation mechanism shows one to two orders of magnitude lower value than the actual weight loss. A new loss mechanism is proposed and discussed in this article.

1. Introduction

Platinum group metals are widely used as catalysts and thermal couple wires under high temperature environments. In the microelectronic industry, platinum and palladium are often used for metallization purpose to make reliable contacts. Because of their many attractive properties at high temperatures, Pt-group metals are usually used in the presence of refractory oxides.

One important property of Pt-group metals to be addressed is their stability at high temperatures when exposed to refractory oxides (glass) environments. It is well recognized that Pt-group metals, such as platinum, rhodium and iridium form various kinds of oxide species under oxidizing atmosphere at elevated temperatures. These precious metal oxides have high vapour pressures and are volatile, which in turn cause the weight loss of precious metal during high temperature service. On the other hand, the real mechanism of precious metal weight loss in a refractory oxide environment is unknown. An important question to consider is does oxidation of Pt-group metals cause the major loss of precious metals in a glass environment. It has come to our attention that SiO_2 itself is detrimental [1] to Pt-group metals, although the real mechanism is not clear. Could a glass environment cause loss of precious metals? Is a glass environment more detrimental than oxygen? To properly address these problems, more understanding about the behaviour of Pt-group metals under a glass environment is necessary.

2. Experimental procedures

High purity Pt–10 wt % Rh samples with dimensions of 1 inch × 1 inch × 0.030 inch were made by Engelhard Corporation. The samples were either unpolished or polished (by alumina slurry or diamond paste) to a surface roughness of about 1 μm, ultrasonically cleaned in acetone (or methanol) and then dried with compressed air before the experiment.

To conduct experiments of precious metal loss in a refractory oxide environment, Pt–Rh plate was annealed under the following conditions: (1) a box furnace with refractory oxides brick (primarily SiO_2, Al_2O_3 and minor amounts of CaO and MgO) at one atmospheric pressure, and (2) a sealed fused quartz tube at a vacuum level of 10^{-2} to 10^{-3} torr. A solid state contact study was also conducted by sandwich-

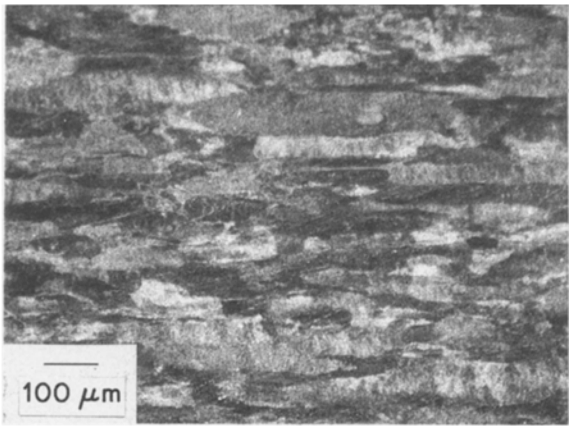

Figure 1 An optical micrograph showing the microstructure of as-received Pt–Rh alloy. A typical mechanical texture due to cold rolling was observed. The sample was electrolytically etched by 100 cm^3 HCl + 15 g NaCl under the condition of 3V (a.c.) for 45 sec.

0022-2461/90 $03.00 + .12

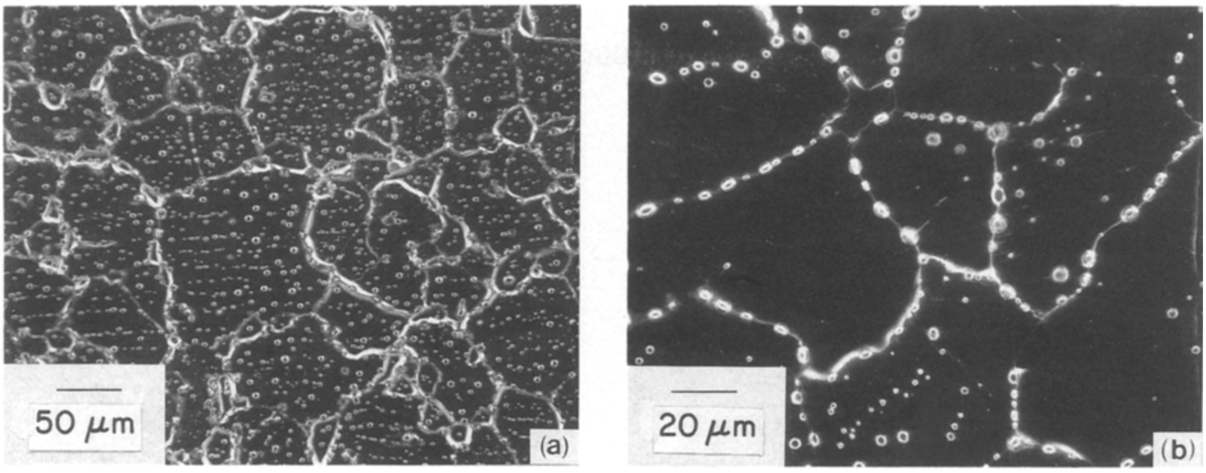

Figure 2 (a) An optical micrograph showing the distribution of surface pits. The sample was annealed in refractory oxides environment. (b) A high magnification optical micrograph showing the grain boundary pits in localized area.

TABLE I Summary of the weight loss of precious metals under various environments at 1300° C

Environments	Weight loss	
	(mg cm^{-2})	(%)
Furnace air	1.6 (60 h)	0.165 (60 h)
	3.1 (100 h)	0.494 (100 h)
	6.4 (150 h)	0.8 (150 h)
SiO_2 plates	–	0.22 (150 h)
Al_2O_3 plates	–	0.14 (150 h)
[5]	0.246 (60 h)	–
	0.615 (150 h)	
[6]	0.0432 (60 h)	–
	0.108 (150 h)	

The annealing time was indicated inside the parentheses. (Literature data were also included for comparison.)

ing Pt–Rh alloy between pairs of α-Al_2O_3 and quartz (SiO_2) plates, and annealed under the condition (1).

The samples were then annealed at 1300° C for 60, 100 and 150 h. Following the annealing, weight loss was measured by a balance. The samples were examined by optical and scanning electron microscopy with energy dispersive X-ray analysis. Scanning Auger microscopy and laser Raman microprobe were applied to identify the surface reaction products.

3. Results

Fig. 1 shows the microstructure of an as-received Pt–Rh alloy. Typical elongated grains due to cold rolling were observed. Table I summarizes the weight loss of precious metal from different experiments.

3.1. Refractory oxides environment

The weight losses were measured to be 0.165, 0.494 and 0.8% after the samples were annealed at 1300° C for 60, 100 and 150 h, respectively. Normalizing these weight losses by their respective surface areas, the kinetics of weight loss per unit surface area ($\Delta W/A$) as a function of annealing time can be established. Based on the present experimental results, the weight loss data can be best described by $(\Delta W/A)^{1/3} = Kt$, where K is the rate constant and t the annealing time.

The sample surface appeared shiny when examined visually. Under an optical microscope, however, the surface was decorated by large numbers of pits, as shown in Fig. 2. These pits were of micrometer in size, and distributed homogeneously along the grain boundaries and inside the grains. In the vicinity of these surface pits, unique feathery-like patterns were found. Under a scanning electron microscope, the feathery-like patterns were characterized by river-like striation patterns, as shown in Fig. 3. The striations

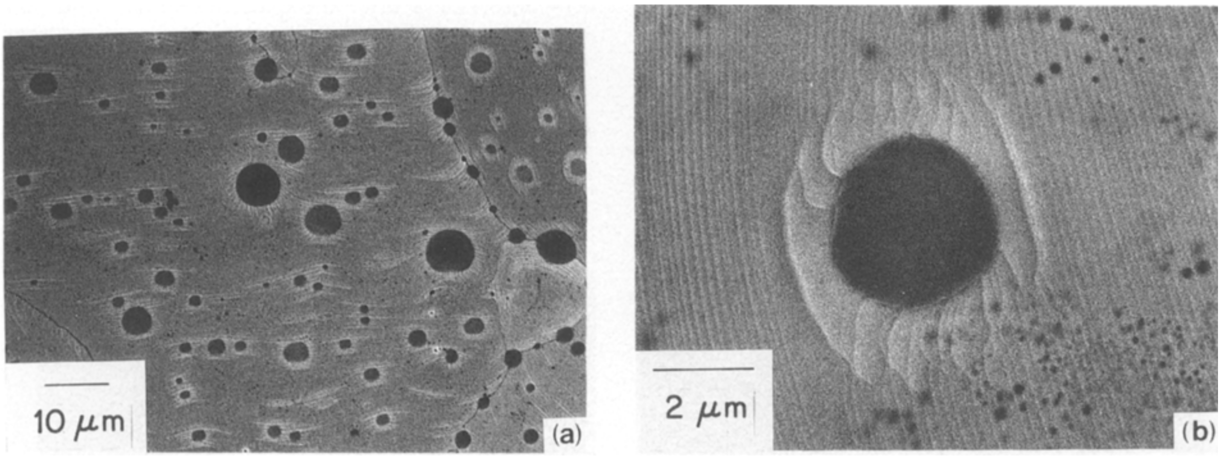

Figure 3 SEM micrographs showing the surface pits and associated striation patterns at (a) low, and (b) high magnifications. At high magnification, it was noted that the circumferential areas around the pits were lower than the remote areas.

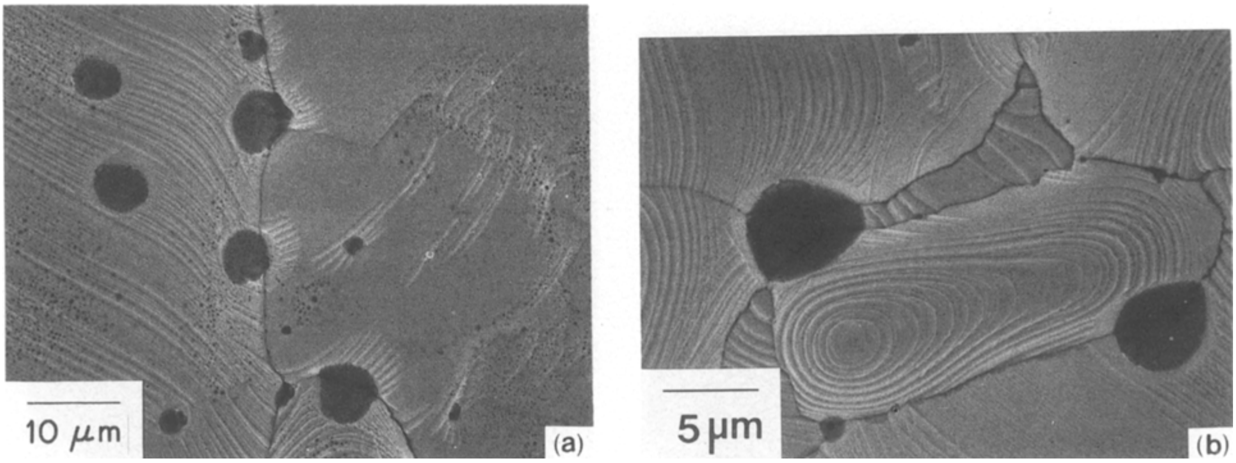

Figure 4 (a) A SEM micrograph showing curved striation patterns associated with the pits which are located along grain boundary. A change of the orientation from one grain into the other was noted. (b) A SEM micrograph showing a typical surface morphology due to surface migration of atoms. Grain boundary grooving was observed, and island-shaped grain was developed.

were discontinuous in nature, and were associated with the pits only. The orientations of these striations were aligned consistently within the same grain. And the orientation changed from one grain to another. Fig. 4a shows curved striation patterns associated with the pits along grain boundaries. Changes in orientation of the striations from one grain into another were observed. Grain boundary grooving due to surface tension effect was noticed. In some of the grains, island-shaped structure was produced, as shown in Fig. 4b.

SEM X-ray microanalysis indicated the surface pits were enriched with silicon and aluminium. Figs 5b and c show SiKα and AlKα X-ray maps, respectively, of the surface pits from an area shown in Fig. 5a. The maps indicate that the pits were enriched with higher silicon concentration than aluminium. It is clear from this experiment that refractory oxides, specifically SiO_2 and Al_2O_3, are harmful to Pt–Rh alloy and they pit surfaces of the alloy.

3.2. Fused quartz environment

Fig. 6 shows an optical micrograph of the surface morphology of Pt–Rh alloy. Large numbers of pits were clearly observed on the sample surface. In addition to that, striation patterns also developed. Figs 7a and b show bright and dark field images, respectively, of the striation patterns. The striation patterns exhibited a unique stacking-fault-like feature under an optical microscope. And they were much more extensively developed than those developed under refractory oxides environment. Most of the patterns extended continuously through the whole grain. In some areas, as shown in Fig. 8, twinning was clearly observed. Symmetrical mirror images of the surface striations with respect to the twinning plane were seen.

Based upon X-ray microanalysis, the pits were found to be enriched with silicon only (no aluminium was detected). Elemental mapping by scanning Auger analysis indicated that the pitted areas were enriched with silicon and oxygen, but depleted of platinum and rhodium, as shown in Fig. 9. Laser Raman microprobe analysis from those pits indicated that α-cristobalite was formed inside the pits. Three Raman peaks of α-cristobalite phase were identified and shown in Fig. 10. However, no PtSi or Pt_2Si were found.

3.3. Solid state contact

The weight losses from Pt–Rh were measured to be 0.14 and 0.22% after the experiments of solid state contact with Al_2O_3 and SiO_2 plates, respectively, at

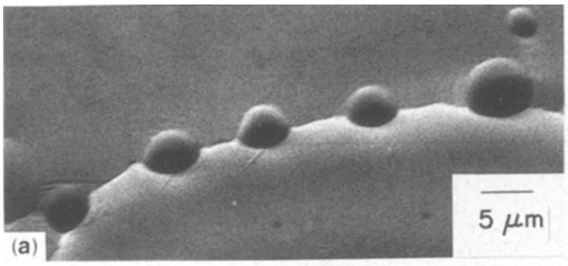

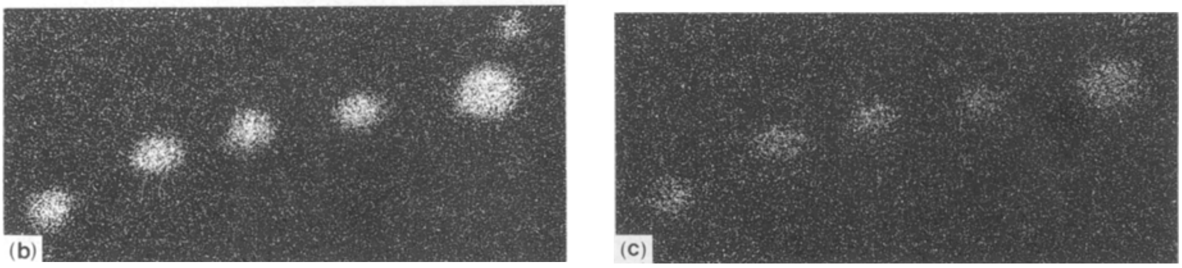

Figure 5 (a) A SEM image, (b) SiKα and (c) AlKα X-ray maps of the surface pits. The pits were found to be enriched with more silicon than aluminium. The sample was exposed to refractory oxides environment at 1300° C for 60 h.

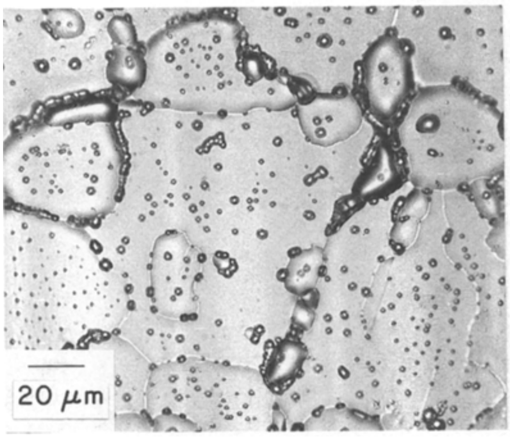

Figure 6 An optical micrograph showing the distribution of surface pits on Pt–Rh. The sample was annealed in a quartz tube under a vacuum level of 10^{-2} to 10^{-3} torr.

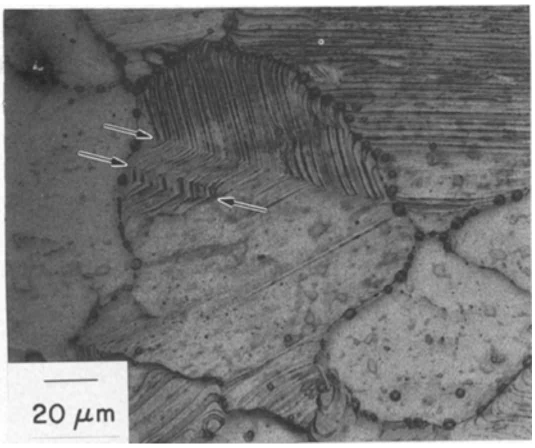

Figure 8 An optical micrograph showing symmetrical mirror images of the surface flow with respect to the twinning plans. The twinning plans were indicated by arrows.

1300° C for 150 h. The values of weight loss are relatively small, as compared to the 0.8% loss generated in the refractory oxides environment, due to the incorporation of SiO_2 and Al_2O_3 into the alloy.

Direct evidence of reactions between Pt–Rh and SiO_2 as well as Pt–Rh and Al_2O_3 were observed. Small pieces of oxides were disintegrated from the oxide plates and fused to the Pt–Rh sample. Under a scanning electron microscope, the reaction zones exhibit different features depending upon the contacting oxide species. Samples in contact with SiO_2 showed a unique reaction pattern. "Orange peel" phenomenon was observed on the Pt–Rh grains under an optical microscope. A SEM micrograph indicated that Pt–Rh grains were divided into many small domains with SiO_2 impregnated into the domain boundaries. As a result, the reaction zone is characterized by hillocks of SiO_2 along the domain boundaries as shown in Fig. 11. Raman microprobe indicated that the SiO_2 existed in either α-cristobalite or amorphous states. On the other hand, samples exposed to Al_2O_3 showed a less extensive and different reaction pattern as compared to those exposed to SiO_2. Dendritic reaction zones were observed and shown in Fig. 12. X-ray mapping showed the reaction zones were enriched with aluminium and oxygen, but depleted of platinum and rhodium.

4. Discussion

By immersing alternating current heated thermocouple wires into loosely packed refractory powders, Darling *et al.* [2–4] reported severe interactions between platinum and refractory oxides, specifically Al_2O_3, ZrO_2 and ThO_2, under reduced oxidizing potential. Nevertheless, they claimed [2] that platinum was exceedingly inert with respect to refractory oxides under normal atmospheric conditions. In the present experiment, however, it is observed that refractory oxides attacked and interacted with Pt–Rh alloy under atmospheric conditions.

The interaction is characterized by pitting and striation patterns. The character of pitting is very similar to corrosion pitting; indicating that refractory oxides may be corrosive to Pt–Rh alloys at high temperatures. The pits are of micrometer in size and exhibit either spherical or elliptical shapes. The pitted area is ubiquitous and contributes to the weight loss of material based upon the calculation from first principles. Loss of Pt-group metals under oxidizing environments has been extensively studied [5–8] and is believed to be due to the formation of volatile oxides, e.g. PtO_2. To our knowledge, loss of Pt-group metals under refractory oxides environments has never been studied before.

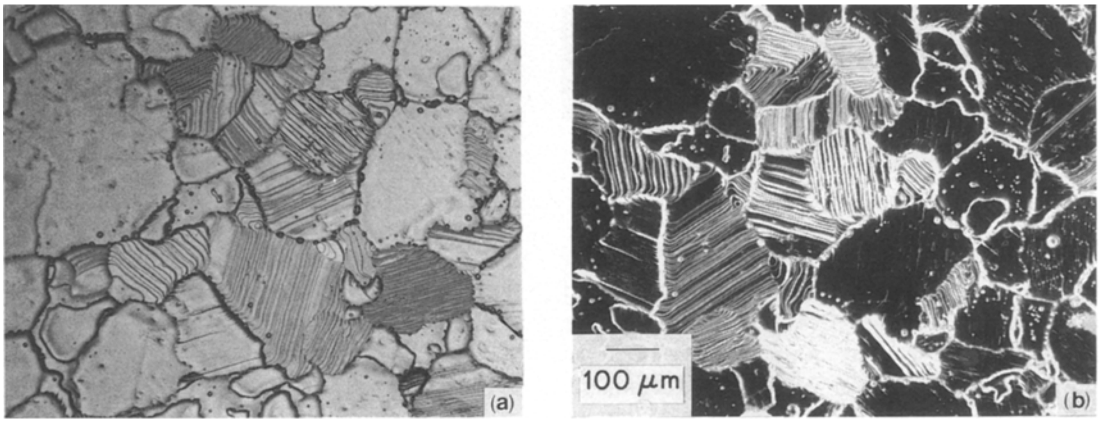

Figure 7 (a) Bright and (b) dark field optical micrographs showing the surface morphologies of Pt–Rh alloy after being exposed to fused quartz environment. A unique stacking-fault-like pattern extended through the whole grains was observed.

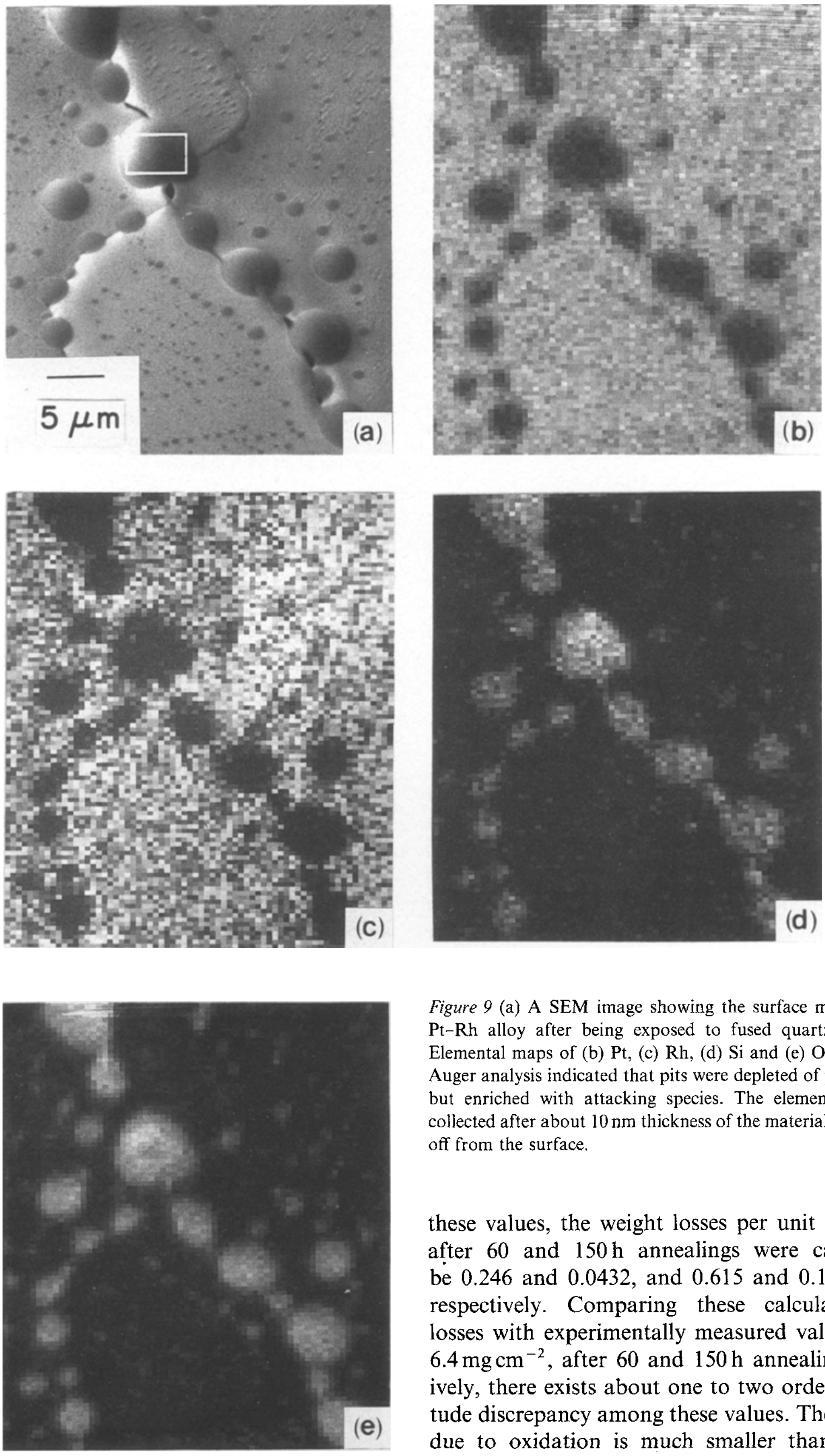

Figure 9 (a) A SEM image showing the surface morphologies of Pt–Rh alloy after being exposed to fused quartz environment. Elemental maps of (b) Pt, (c) Rh, (d) Si and (e) O from scanning Auger analysis indicated that pits were depleted of precious metals but enriched with attacking species. The elemental maps were collected after about 10 nm thickness of the material was sputtered-off from the surface.

To clarify the mechanism of weight loss under refractory oxides environment, the weight loss of precious metals from the present experiments are compared with those that were calculated from literature data based on an oxidation mechanism. The rates of weight loss of Pt–Rh due to oxidation were reported to be about 4.1×10^{-3} [5] and 7.2×10^{-4} mg cm^{-2} h^{-1} [6] at 1300° C under 1 atm. Based on these values, the weight losses per unit surface area after 60 and 150 h annealings were calculated to be 0.246 and 0.0432, and 0.615 and 0.108 mg cm^{-2}, respectively. Comparing these calculated weight losses with experimentally measured values, 1.6 and 6.4 mg cm^{-2}, after 60 and 150 h annealings, respectively, there exists about one to two orders of magnitude discrepancy among these values. The weight loss due to oxidation is much smaller than the actual weight loss in a refractory oxide environment. If added weight from the attacking species of SiO_2 and Al_2O_3 were taken into account, the difference would be even greater. Obviously, an oxidation mechanism alone cannot satisfactorily explain the weight loss in a refractory oxide environment.

Furthermore, if the weight loss of precious metal is governed by an inward diffusion of oxygen, a parabolic relationship of $(\Delta W/A)^n = Kt$ with $n = 2$ would normally be expected. In the present experimental

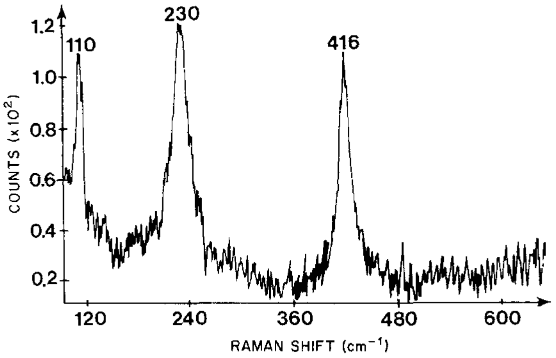

Figure 10 Raman spectrum, as indicated by Raman shifts at 110, 230 and 416 cm^{-1}, showing the primary existing phase in the pits is α-cristobalite.

results, however, $n = 1/3$ gives the best fit of the data, indicating that an inward diffusion of oxygen is not a rate limiting step for the precious metal loss.

Nevertheless, one might argue that the pits could be formed through supersaturation (condensation) of defects, e.g. vacancies and dislocations, which were generated by a large plastic deformation during cold rolling. If this is the case, then high values of the weight loss cannot be explained by the law of mass conservation. Based upon the fact that the formation of the pits, which contributes to the weight loss of Pt–Rh, cannot be reasoned by either oxidation loss or vacancy condensation, a reasonable explanation is that pitting is the characteristic of the interactions between Pt–Rh and refractory oxides.

From the present experimental results, it is believed that both the solid and gaseous phases of refractory oxides can serve as attacking species to Pt–Rh alloy. The liquid phase is also expected to be harmful, although it has not yet been studied. At this moment, it is not clear through what form Pt–Rh was lost. There are two possibilities, however, can be visualized. The first one involves the dissociation of oxygen from refractory oxides followed by interaction with Pt–Rh to form low melting point phases [2]. However, by laser Raman spectroscopy, the major compound formed in the pits was identified to be α-cristobalite. No complex phases consisting of silicon, aluminium and Pt–Rh were found in the pits. The second possibility involves the refractory oxides, in the presence of Pt–Rh, as oxygen media, through which oxygen can be effectively transported from the environment and adsorbed on to the sample, then form volatile oxides. This should be treated differently from an ordinary oxidation from a kinetics viewpoint. To check the validity of this proposal, thermodynamic calculations on the stabilities of SiO_2 dissociation reaction as well as PtO_2 formation reaction need to be conducted.

An intriguing phenomenon observed during this study is the nucleation of striation patterns from the pit. The possibility of striations being formed through chemical etching along certain preferred orientations by oxide species is ruled out based on scanning Auger analysis. No silicon and aluminium species were detected from the striations. It is believed that the striation shows the fingerprint of surface migration of platinum and rhodium atoms. It is well established that surface diffusion is a thermally activated kinetic process which is very sensitive to surface energy. As a result, crystallographic dependence of the striation patterns on grain orientations was observed.

It is suggested that, once the pits form, atoms of platinum and rhodium migrate away from the pits along preferred low energy crystallographic paths. The driving force for atomic migration is believed to be due to the higher chemical potential of the pits. As a result, striation patterns are nucleated from the pits and progressively developed along certain orientations. Concurrently, the areas in the neighbourhood of pits are continuously depleted of platinum and rhodium and the surface level is lowered. As a result, the diameter of the pits grows and the striations gradually extend through the whole grain. The surface migrating Pt–Rh atoms are believed to form volatile oxides species which evaporate effectively, which in turn causes a prevailing weight loss. Similar kinds of

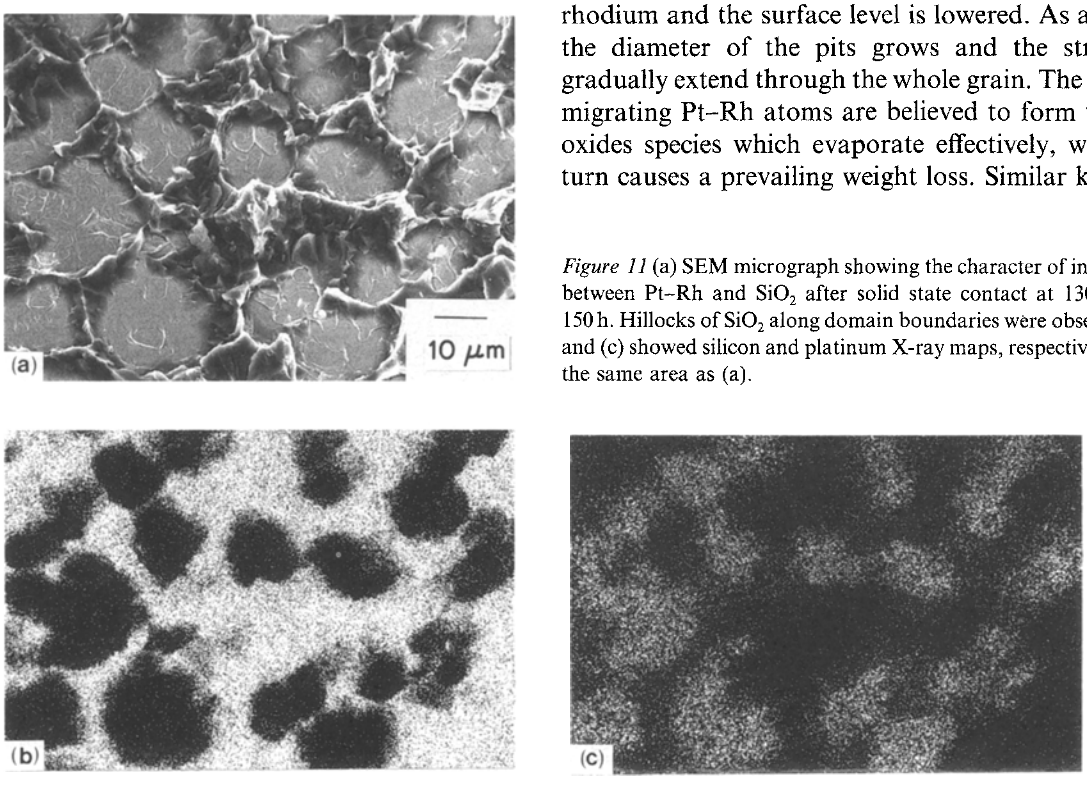

Figure 11 (a) SEM micrograph showing the character of interaction between Pt–Rh and SiO_2 after solid state contact at 1300° C for 150 h. Hillocks of SiO_2 along domain boundaries were observed. (b) and (c) showed silicon and platinum X-ray maps, respectively, from the same area as (a).

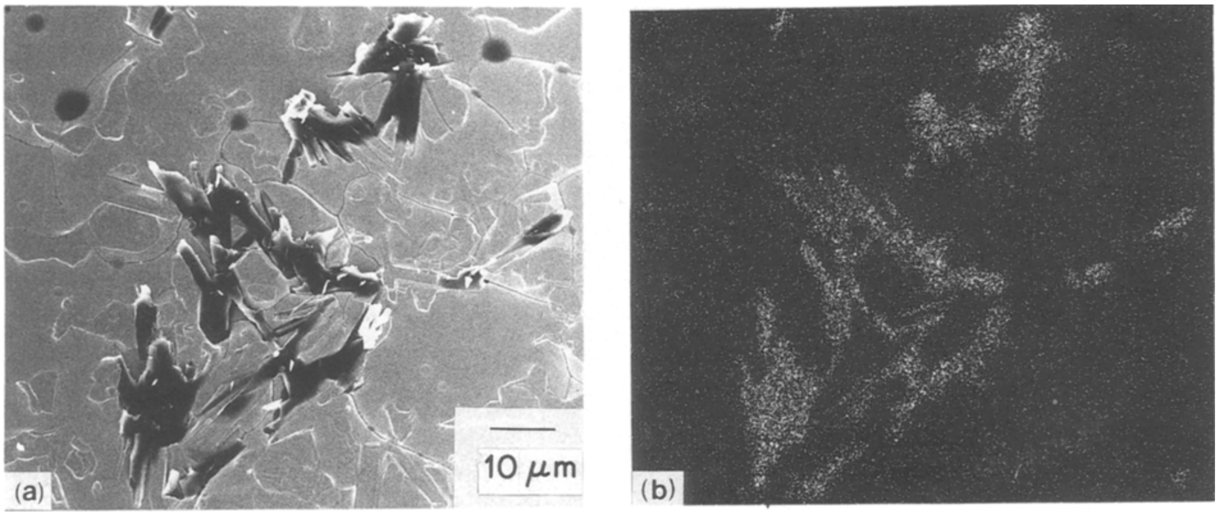

Figure 12 (a) SEM micrograph showing the characteristic of interactions between Pt–Rh and Al_2O_3 after solid state contact at 1300° C for 150 h. Dendritic reaction zones were observed. (b) Al X-ray map indicated that those areas were enriched with aluminium.

striation patterns were also observed on osmium (Os) [5] during an oxidation study. Nevertheless, no description and discussion were available.

5. Conclusion

The weight loss of Pt–Rh alloy was studied under refractory oxides environments, specifically SiO_2 and Al_2O_3. Typical surface interactions, characterized by pits and striations, were observed. Both scanning Auger and energy dispersive X-ray analyses showed the pits were enriched with silicon, aluminium and oxygen; but depleted of platinum and rhodium. Laser Raman spectroscopy identified a reaction product of α-cristobalite in the pits.

SiO_2 species, rather than Al_2O_3, was determined to be more detrimental to Pt–Rh alloy through the observations of (1) more extensive solid state interactions with Pt–Rh, and (2) the development of more extended surface striations on Pt–Rh.

Based upon the calculations, the weight loss due to an oxidation mechanism alone showed at least one order of magnitude discrepancy as compared to the actual weight loss. It is suggested that pitting due to interactions between refractory oxides and Pt–Rh is responsible for the loss of the metals. The surface pits serve as nucleation sites for the later stage development of striation patterns which are due primarily to surface migration of atoms. The surface migrating platinum and rhodium atoms, which give rise to the growth of pits, form volatile oxides species effectively and cause a subsequent weight loss.

Acknowledgements

We are grateful to Z. Gutierrez for the technical support, and to J. Jean and G. Rice for stimulating discussion. Scanning Auger analysis by R. Moore at Perkin Elmer Physical Electronics Laboratory, and Raman microprobe analysis by F. Adar at Instruments SA, Inc. are acknowledged.

References

1. S. HILDEBRANDT, private communication.
2. A. S. DARLING, G. L. SELMAN and R. RUSHFORTH, *Platinium Metals Review* **14** (1970) 54.
3. *Idem, ibid.* **14** (1970) 95.
4. *Idem, ibid.* **14** (1970) 124.
5. C. A. KRIER and R. I. JAFFEE, *J. Less-Common Metals* **5** (1963) 411.
6. C. B. ALCOCK and G. W. HOOPER, *Proc. R. Soc. A* **254** (1960) 551.
7. G. C. FRYBURG and H. PETRUS, *J. Electrochem. Soc.* **108** (1961) 496.
8. J. L. MODISETTE and D. R. SCHRYER, NASA TN D-222 (March, 1960).

Received 22 December 1988
and accepted 20 June 1989